Effect of internal radiation on the crystal-melt interface shape in Czochralski oxide growth

O.N.Budenkova[a], V.M.Mamedov[a], M.G.Vasiliev[a], V.S.Yuferev[a], Yu.N.Makarov[b]

[a] A.F. Ioffe Physico-Technical Institute, Russian Academy of Sciences,
26 Politekhnicheskaya st., St.Petersburg 194021, Russia
Tel.: +7-812-247-9175; Fax: +7-812-247-10-17; E-mail: olganb@mail.ioffe.ru

[b] USA Semiconductor Technology Research, Inc.,
P.O. Box 70604, Richmond, VA 23255-0604, USA;
Tel.: +1-804-304-8092; Fax: +1-804-217-70-76; E-mail: yuri.makarov@semitech.us

Introduction.

Most oxide crystals (BGO, BSO, BTO, YAG, GGG) display transparency to infrared radiation that can greatly influence the crystal-melt interface shape during Czochralski growth since an additional mechanism arises for a heat removal from the vicinity of the crystallization front. Additional important factor affecting upon the shape of solid/liquid interface is related to the **Fresnel's reflection** (refraction) at **the transparent crystal surface** [1].

In practice:

1. The shape of real crystals can be appreciably differed from a regular cylinder or a cone that has to lead to scattering of radiation at the crystal surface and, consequently, to smoothing of the radiation heat flux distribution at the melt/solid interface.
2. Many oxide crystals demonstrate the pronounced tendency toward faceting of the solidification front that imply considerable supercooling at the facetted interface which should be taken into account in global simulation.

Note:

Up to now numerical calculation of facet formation was performed only for Bridgman process and internal radiation transport was treated using either the Rosseland diffusion approximation [2] or P_1-approximation [3]

The objectives of the modeling:

1. To investigate the influence of deflections in the shape of a real crystal from conical and cylindrical geometry on the distributions of radiative heat flux over the crystallization front.
2. To investigate the effect of internal radiation and Fresnel reflection at the crystal surface on the process of facet formation in Cz oxides growth.

As a representative growth process, the $Bi_4Ge_3O_{12}$ low-thermal gradients Cz growth was considered (see Fig.A).

Characteristics of growth process

Melting temperature: T_m=1323 K

Radiative and thermal properties of the crystal:

- Thermal conductivity: κ_S=1.2 W/(m·K)
- Refractive index n=2.15
- Absorption coefficient k is approximated by three-bands model:

λ<4μm	k=3.0 m^{-1}
4<λ<6μm	k=95.5 m^{-1}
λ >6 μm	k=∞

- Crystal cone angle α=45°
- Radiative properties of other materials:
- Crucible emissivity (platinum): ε_C=0.15
- Emissivity of a free melt surface: ε_L=0.18

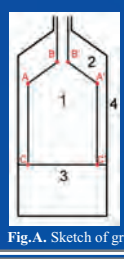

1 – crystal, 2 – gas gap, 3 – melt, 4 – crucible.

Fig.A. Sketch of growth set-up.

Calculation of reflection coefficients

Reflection coefficients for Fresnel's reflection is calculated by Fresnel formulae. For diffuse reflection they are obtained from the latter by averaging over the angle of incidence [4] (Fig.B).

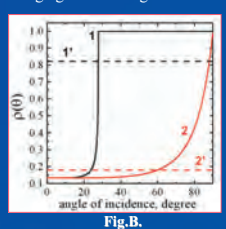

Fig.B.

1 – coefficient of specular reflection for radiation incident on the crystal surface from the crystal;

1' – coefficient of diffuse reflection for radiation incident on the crystal surface from the crystal;

2 – coefficient of specular reflection for radiation incident on the crystal surface from gas;

2 – coefficient of diffuse reflection for radiation incident on the crystal surface from gas.

Description of the problem

Radiative problem for the crystals with perturbed surfaces and flat crystallization front was solved. The actual (known from the experiment) temperature distribution over the crucible wall was used as a boundary condition.

Results of the calculations are presented in Fig.1.1-1.5 and 2.1-2.5 in a view of temperature fields in the crystal and heat flux $\boldsymbol{q}$ removing from the crystallization front (see Fig. 1.6 and 2.5):

$$q = \mathbf{q}\cdot\mathbf{e}_z = \left(-\lambda\frac{\partial T}{\partial n}\Big|_S + q_{rad}\right)\cdot\mathbf{e}_z$$

where q_{rad} is the density of the net radiative flux at the solid-melt interface in the range of semi-transparency of the crystal.

Description of disturbances:

Radial disturbance of the crystal side surface (see Fig.1.1-1.5) were given in the following form:

$$R = R_0 + \varepsilon_1 \sin\frac{2\pi n_1}{L}z$$

Perturbations on the conical part of the crystal side surface (see Fig.3.1-3.5) were given as follows:

$$Z = R_0\cot\alpha + z_* - r\cot\alpha - \frac{\varepsilon_2}{\sin\alpha}\sin\frac{2\pi n_2 r}{R_0}$$

where:

R_0 – base radius of a crystal
R – current radius of a crystal for wave perturbations.
ε_1, ε_2 – perturbation amplitude
L – crystal length
n_1, n_2 – numbers of periods of perturbations on the surface
α – cone angle

I.1 Effect of deflection of a cylinder's generatrix from a straight line.

From cases 1 to 4 specular reflection takes place both on the conical and cylindrical surfaces. For the case 5 reflection on the conical part of crystal surface is specular and on the cylindrical one is diffuse.

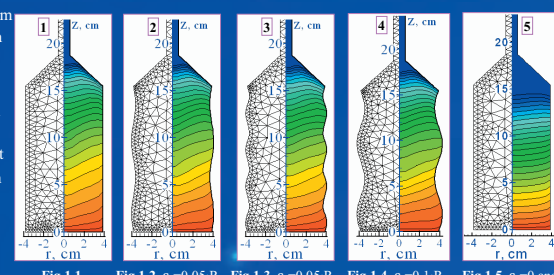

Fig 1.1. ε_1=0

Fig 1.2. ε_1=0.05·R_0 (ε_1=0.1925 cm) n_1=2

Fig 1.3. ε_1=0.05·R_0 (ε_1=0.1925 cm) n_1=4

Fig 1.4. ε_1=0.1·R_0 (ε_1=0.385 cm) n_1=2

Fig 1.5. ε_1=0 and diffuse reflection on cylindrical surface.

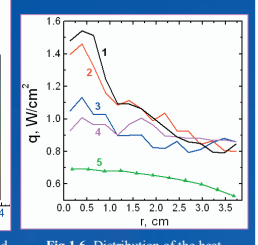

Fig.1.6. Distribution of the heat flux in solid phase over the crystallization front for the cases 1-5 shown on the left.

Resume:

Deflections of crystal lateral surface from a cylinder with straight generatrix can result to significant smoothing of the radiation heat flux distribution at the solid/liquid interface.

Therefore: wavier crystal's cylindrical surface leads to the flatter crystallization front.

I.2 Effect of deflection of shoulder side surface from a regular conical form

From cases 1 to 3 specular reflection takes place both on the conical and cylindrical surfaces. For the case 4 reflection on the conical part of crystal surface is diffuse while on the cylindrical one is Fresnel's .

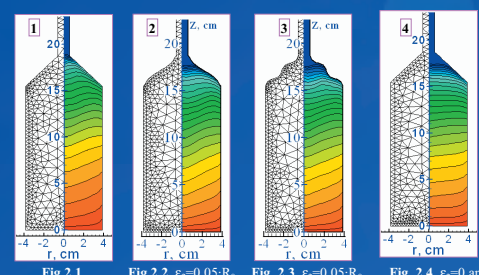

Fig.2.1. ε_2=0

Fig.2.2. ε_2=0.05·R_0 (ε_2=0.1925 cm) n_2=1

Fig. 2.3. ε_2=0.05·R_0 (ε_2=0.1925 cm) n_2=2

Fig. 2.4. ε_2=0 and diffuse reflection on conical surface.

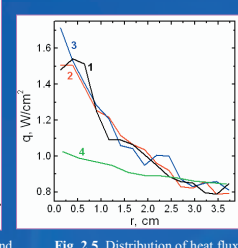

Fig. 2.5. Distribution of heat flux in solid phase over the crystallization front for the cases 1-4 shown on the left.

Resume

Deflections of shoulder surface from a regular conical shape do not change the radiation heat flux distribution along the solid/liquid interface.

Specific feature in the approach to the calculation of facetted front.

In the suggested algorithm a facet is approximated by a planes since small deflection of a facet from a close-packed surface does not influence on the heat transfer processes.

In this case a single parameter is needed (with the exception of crystallographic orientation of the facet) to define the position of the facet on the crystallization front and its size. In suggested algorithm the value of maximal supercooling is selected as this parameter.

Described approach is a numerical expansion of the analytical one suggested in [5].

I. Results of simulation for Fresnel's reflection in the absence of cylindrical part of the crystal.

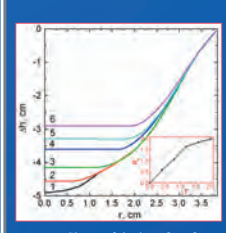

Fig.1. Shape of the interface for ΔTmax: 1 - 0K; 2 - 0.45K; 3 - 0.8K; 4 - 1.2K; 5 - 1.6K; 6 -1.8K. Involved graph: dependence of radius of a facet on the supercooling ΔTmax

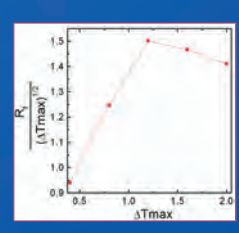

Fig.2. Dependence of relation $R_f / \sqrt{\Delta T_{\max}}$ on $\Delta T_{\max}$

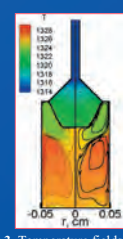

Fig.3. Temperature fields in the crystal and the melt (left) and streamlines in the melt (right) for calculated shape of the interface for ΔTmax=1.2K

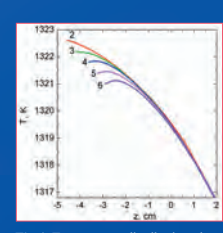

Fig.4. Temperature distribution along the axis of symmetry in the crystal for different values of ΔTmax: 1 – 0 K; 2 - 0.45 K; 3 - 0.8K; 4 - 1.2K; 5 - 1.6K; 6 -1.8K

II. Results of simulation for Fresnel's reflection on the shoulder's surface (AB - A'B' shown in Fig.A) and diffuse on the cylindrical one (CA - C'A' shown in Fig.A).

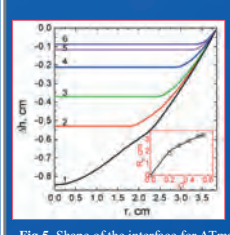

Fig.5. Shape of the interface for ΔTmax: 1 - 0K; 2 - 0.2K; 3 - 0.2K; 4 - 0.4K; 5 – 0.5K; 6 - 0.55K. Involved graph: dependence of radius of a facet R_f on the supercooling ΔTmax

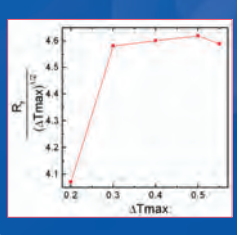

Fig.6. Dependence of relation $R_f / \sqrt{\Delta T_{\max}}$ on $\Delta T_{\max}$

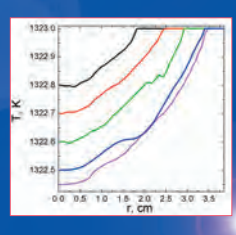

Fig.7. Temperature distribution over the interface for different supercooling ΔTmax

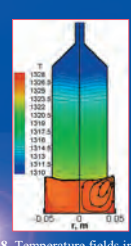

Fig.8. Temperature fields in the crystal and the melt (left) and streamlines in the melt (right) for calculated shape of the interface for ΔTmax=0.3K

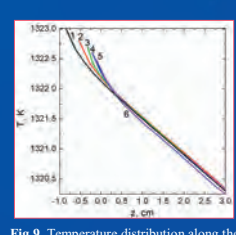

Fig.9. Temperature distribution along the axis of symmetry in the crystal for different values of supercooling ΔTmax: 1 - 0K; 2 - 0.2K; 3 - 0.2K; 4 - 0.4K; 5 - 0.5K; 6 -0.55 K

III. Results of simulation for Fresnel's reflection on the whole crystal side surface.

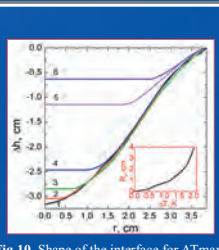

Fig.10. Shape of the interface for ΔTmax: 1 - 0K; 2 - 0.45K; 3 - 0.8K; 4 - 1.2K; 5 - 1.6K;6 -1.8K. Involved graph: dependence of radius of a facet R_f on the supercooling ΔTmax

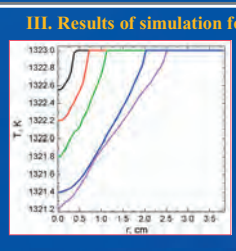

Fig.11. Temperature distribution over the interface for different supercooling ΔTmax

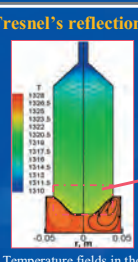

Fig.12. Temperature fields in the crystal and the melt (left) and streamlines in the melt (right) for calculated shape of the interface for ΔTmax=1.2K

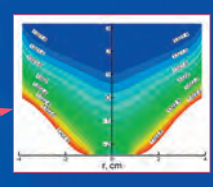

Fig.13. Temperature fields in the crystal near the crystallization front for ΔTmax=1.2K

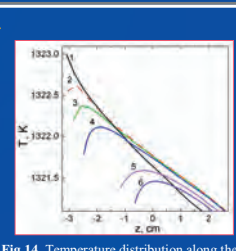

Fig.14. Temperature distribution along the axis of symmetry in the crystal for different values of supercooling ΔTmax: 1 - 0K; 2 - 0.45 K; 3 - 0.8 K; 4 - 1.2 K; 5 - 1.6 K; 6 -1.8K

IV. Results of simulation of a set of oblique facets.

Inclined facets require 3D simulation both for liquid and solid phase. However, in the present work the system of inclined facets was replaced by a "conical facet". In **Fig.15a-c** results of simulation of facets {112} are presented.

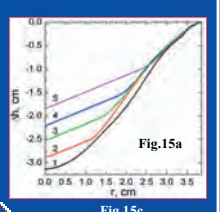

Fig.15a

Fig.15a: Shape of the interface for ΔTmax: 1 - 0K; 2 - 0.4K; 3 - 0.8K; 4 - 1.2K; 5 - 1.4K

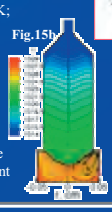

Fig.15b

Fig.15b: Temperature fields in the crystal and the melt (left) and streamlines in the melt (right) for calculated shape of the interface for ΔTmax=1.2K

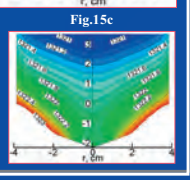

Fig.15c

Fig.15c: Temperature fields in the crystal near the crystallization front for ΔTmax=1.2K

Chart of calculation procedure of the interface shape with the horizontal flat (central) facet:

Input parameter is ΔTmax

Start of the calculation

↓

Determination of facet radius R_f^k for current (fixed) shape of interface $h_k(r)$

↓

Calculation of RCT problem inside the crystal and gas gap above the melt (domains 1, 2). Boundary conditions at the interface are of the **first kind:**

$$T_L = T_m - \Delta T_{\max} \quad if \quad r = 0$$
$$T_S(r) = T_m \quad R_f^k < r \le R_0$$
$$T_S(r) = T^i(r) \quad 0 < r \le R_f^k$$

↓ Transfer of obtained values of heat fluxes: $q^i_{rad}(r)$ $q^i_S(r) = -\kappa_S \mathbf{n}\cdot\nabla T_S$

Calculation of convection and heat transfer in the melt (domain 4). At the interface boundary conditions of **mixed type** are used:

$$T_L(r) = T_m - \Delta T_{\max} \quad if \quad r = 0$$
$$T_L(r) = T_m \quad R_f^k < r \le R_0$$
$$\kappa_L \mathbf{n}\cdot\nabla T_L^i = L(\mathbf{n}\cdot\mathbf{e}_z)V_{GR}^i(0) - q^i_{rad}(r) - q^i_S(r) \quad 0 < r \le R_f^k$$

where $V_{GR}^i(0) = \dfrac{-\kappa_L \mathbf{n}\cdot\nabla T_L^i(0) - q^i_{rad}(0) - q^i_S(0)}{L(\mathbf{n}\cdot\mathbf{e}_z)}$

↓

Checking of convergence of a temperature at the facet:

$0 < r \le R_f^k \quad |T^i(r) - T^{i-1}(r)| < \varepsilon$?

No → i=i+1

↓ Yes

Correction of the shape of crystallization front, taking into account that:

1.Facet moves as a single whole

2.Triple point is a stationary one.

$$\frac{dh^k}{dt} = V_{GR}(0) - V_{GR}(R_0) \quad 0 \le r \le R_f^k$$
$$\frac{dh^k}{dt} = \frac{\kappa_L \mathbf{n}\cdot\nabla T_L - \kappa_S \mathbf{n}\cdot\nabla T_S - q_{rad}}{L(\mathbf{n}\cdot\mathbf{e}_z)} - V_{GR}(R_0) \quad R_f^k < r \le R_0$$

↓

Checking, whether the growth rate is the same over the crystallization front, both for facetted and rough parts (quasi-stationary state)?

No → k=k+1

↓ Yes

Completion of calculations

Conclusions:

Part I.

- The influence of the deflections in the shape of a crystal on the radiative heat removal from melt/liquid interface is investigated as applied to the $Bi_4Ge_3O_{12}$ low-thermal gradients Cz method.
- It is shown that perturbations of the specular cylindrical part of crystal surface can be replaced by the diffuse reflective unperturbed surface.
- On the other hand, the shoulder surface of oxide crystals has to be treated as a specular one both in unperturbed and perturbed cases.

Acknowledgement: The work was supported by INTAS, number INTAS 00-263.

Part II.

1. The algorithm of calculation of the faceted solid/liquid interface in Cz process along with RHT process is suggested.
2. It is shown that for the case of low front's convexity (when the crystal's cylindrical surface is diffuse reflecting) the effect of radiative transfer turns out insignificant.
   The dependence of the size of a facet for this case appears to be close to the known root law [6].
   $$R_f \sim \sqrt{\Delta T_{\max}}$$
3. For the cases of large convexity of the melt/liquid interface (the case of specular reflection) the effect of internal radiation on the facet formation turns out very significant.
   In this case RT leads to the appearance of bottleneck temperature field in crystal and to a more strong dependence of the facet size on supercooling than the root law

1. V.S.Yuferev, O.N.Budenkova, M.G.Vasiliev, S.A.Rukolaine et al, *J. Cryst.Growth, 253 (2003) 383.*
2. Y. Liu, A.Virozub, S.Brandon, *J. Crystal Growth 205 (1999) 333.*
3. C.W. Lan, C.Y. Tu, Y.F. Lee, *Int. J. of Heat and Mass Transfer 46 (2003) 1629.*
4. Ozisik M.N. "Radiative transfer and interactins with conduction and convection", 1975, A Willey-Interscience Publication.
5. V.S.Yuferev, E.Kh. Lokharu , J. Technical Physics, *54 (1984) 1685 (in Russian)*
6. V.V.Voronkov, Crystallography, *17 (1972) 909 (in Russian).*